

Entropic sampling in the path integral Monte Carlo method

P N Vorontsov-Velyaminov¹ and A P Lyubartsev²

¹ Molecular Biophysics Department, Faculty of Physics, University of Saint Petersburg, 198504 St Petersburg, Russia

² Division of Physical Chemistry, Arrhenius Laboratory, Stockholm University, S-106 91 Stockholm, Sweden

E-mail: voron.wgroup@pobox.spbu.ru

Received 16 August 2002, in final form 21 November 2002

Published 7 January 2003

Online at stacks.iop.org/JPhysA/36/685

Abstract

We have extended the entropic sampling Monte Carlo method to the case of path integral representation of a quantum system. A two-dimensional density of states is introduced into path integral form of the quantum canonical partition function. Entropic sampling technique within the algorithm suggested recently by Wang and Landau (Wang F and Landau D P 2001 *Phys. Rev. Lett.* **86** 2050) is then applied to calculate the corresponding entropy distribution. A three-dimensional quantum oscillator is considered as an example. Canonical distributions for a wide range of temperatures are obtained in a single simulation run, and exact data for the energy are reproduced.

PACS numbers: 02.70.Ss, 05.20.Gg, 05.30.-d

1. Introduction

In the last decade Monte Carlo simulation in generalized ensembles such as expanded ensemble [1–4], simulated [5] and parallel tempering [6], multicanonical [7] and entropic [8] sampling has become an important tool in solving various complicated problems of molecular and statistical physics (for example, see a recent review by Iba [9]). Common to these approaches is some modification of statistical ensembles, aimed at overcoming certain difficulties or limitations of conventional Monte Carlo or molecular dynamics methods. Such difficulties usually arise when a standard simulation algorithm is unable to sample properly all relevant regions of the configurational space, as is the case for free energy computations or when the configurational space is separated into different parts with a slow transition rate between them. Generalized ensembles modify the original, typically canonical, ensemble in a way which improves sampling of the relevant region of configurational space. A characteristic example is the temperature-expanded ensemble when one joins low- and high-temperature

configurations. Besides improvement of sampling, the generalized ensemble algorithms often allow one to estimate various thermodynamic properties over a wide range of temperatures (or other parameters) from a single simulation run.

An important algorithmic point in most of these approaches is the problem of initial estimation and further adjustment of the so-called balancing factors, which regulate the resulting probability distribution and are extremely important for the success of the method. For example, in the expanded ensemble method it is necessary to obtain a nearly flat distribution of visits to separate subensembles. In the entropic sampling, one needs to get a flat distribution over energy. In very recent works [10, 11] Wang and Landau suggested an algorithm which provides an automatic adjustment and accurate finetuning of relevant parameters.

So far the discussed methods were used for simulation of either lattice models or continuous classical systems. In this work we apply the entropic sampling [8] within the Wang–Landau algorithm to calculate the density of states in the canonical quantum partition function. It is known that a quantum particle at finite temperature can be presented, within the path integral formalism [12], as a ‘ring polymer’ consisting of n beads connected by harmonic bonds (springs) [13, 14]. The springs, however, become very stiff at high temperatures or at great number of beads n . This leads to numerous difficulties in practical simulations by the conventional canonical Monte Carlo algorithm, related to the slow sampling of the configurational space. The situation becomes more severe for many interacting quantum particles. The problem thus falls in the class where generalized ensemble methods have proved to be useful.

The aim of this paper is to present the entropic sampling approach in the case of quantum statistics. We demonstrate the method on a simple example of a three-dimensional quantum oscillator. While simulation of a quantum oscillator does not pose a computational problem in a conventional path integral Monte Carlo scheme, the example is instructive because it allows comparison with the exact analytical solution. Moreover, it allows one to obtain some interesting insights into the machinery behind the path integral Monte Carlo technique.

2. Entropic sampling for quantum partition function

The path integral form of the canonical quantum partition function $Z(\beta)$ in the n -bead approximation can be expressed as

$$Z_n(\beta) = \int dq \exp\left(-\frac{H_1(q)}{\beta} - \beta H_2(q)\right). \quad (1)$$

Here q is a dNn -vector (d —dimensionality, N —number of particles, n —number of beads); $\beta = (kT)^{-1}$ is the reciprocal temperature; and $H_1(q)$ and $H_2(q)$ are temperature-independent functions of coordinates:

$$H_1(q) = \frac{n\mu}{2\hbar^2} \sum_{1 \leq t \leq n} (r_t - r_{t+1})^2 \quad (2)$$

(r_t is a dN dimensional vector, μ is the mass of a particle, $r_{n+1} \equiv r_1$) and

$$H_2(q) = \frac{1}{n} \sum_{1 \leq t \leq n} V(r_t). \quad (3)$$

$H_1(q)$ is related to the kinetic energy of the system and $H_2(q)$ accounts for the potential energy. The latter in the general case includes both external field and interparticle interactions.

Reciprocal temperature β enters into two terms of the exponent in (1) in different (inverse) powers, 1 and -1 . Hence the density of states, Ω , which we are now going to introduce, would necessarily depend on two variables, E_1 and E_2 . We can present $Z_n(\beta)$ in (1) as

$$Z_n(\beta) = \int dE_1 dE_2 \exp\left(-\frac{E_1}{\beta} - \beta E_2\right) \Omega(E_1, E_2) \quad (4)$$

where

$$\Omega(E_1, E_2) = \int dq \delta(E_1 - H_1(q)) \delta(E_2 - H_2(q)) \quad (5)$$

is the density of states independent of temperature. The range for E_1 in (4) is always positive while E_2 can generally have both signs.

Unfortunately $\Omega(E_1, E_2)$ cannot be reduced to a product of two terms depending separately on E_1 and E_2 . So, in contrast to the case of classical statistics, we meet with a two-variable problem. In other aspects it is an analogue of the classical density of state function. In order to avoid large numbers we deal with the logarithm of Ω , which can be regarded as corresponding to the ‘entropy of states’ or entropy distribution, $S(E_1, E_2) = \ln \Omega(E_1, E_2)$. Knowing Ω (or S), one gets the canonical distribution function

$$P(E_1, E_2; \beta) = \exp(-E_1/\beta - E_2\beta + S(E_1, E_2)) \quad (6)$$

from which all thermodynamical properties can be obtained.

It should be noted here that the normalization constant for Ω is important only for the calculation of the partition function itself while averages such as the potential or kinetic part of the internal energy are independent of any additional factor since the latter enters integrals in both the numerator and denominator of the relevant expressions and cancels.

Practical simulations have been carried out for a three-dimensional quantum oscillator so that $V(r) = \frac{\mu\omega^2}{2}r^2 > 0$ and the area of integration in (4) is restricted to the positive values of both E_1 and E_2 . The number of beads in most calculations was set to $n = 5$, additional simulations have been made for $n = 8$. Calculations were carried out in a rectangle (mainly in a square) with $0 < E_1 < E_{\max 1}$, $0 < E_2 < E_{\max 2}$. A grid of cells (boxes) labelled by (i, k) , $1 \leq i \leq N_{b1}$, $1 \leq k \leq N_{b2}$, was introduced. We use natural oscillator units in which energy is measured in $\hbar\omega$ and distance in $\sqrt{\hbar/(\mu\omega)}$. In these units $H_1(q) = \frac{n}{2} \sum_{1 \leq i \leq n} (r_i - r_{i+1})^2$ and $H_2(q) = \frac{1}{2n} \sum_{1 \leq i \leq n} r_i^2$.

Following the Wang–Landau algorithm [10, 11], we equate to zero all initial values of entropy distribution, S_{ik} , corresponding to (i, k) cells. Each MC step includes variation of coordinates of a uniformly chosen arbitrary bead and an attempt to shift it to a new position. If the trial energy pair, $(E_1, E_2)_{\text{tr}}$, does not leave the energy rectangle, the transition is determined according to the following probability rule: $p(ik \rightarrow i'k') = \min(1, \exp(S_{ik} - S_{i'k'}))$. In all other cases the trial configuration is rejected. Irrespective of acceptance of the trial state, a constant, Δs , is added to the current entropy value (i.e. either to the previous, S_{ik} , or to the newly accepted one, $S_{i'k'}$). The number of visits counter ($nv(i, k)$ or $nv(i', k')$ correspondingly) is augmented by 1. For the initial value of Δs we mainly used (in accordance with [10]) $\Delta s = \Delta s_0 = 1$, but other initial values Δs_0 can be chosen as well. The length of a single MC sweep, m , was taken equal to several million elementary steps so as to provide an average number of visits throughout a sweep to each energy cell of about several hundred. The second sweep of the same length (and all further sweeps) started with a modification of Δs : $\Delta s \rightarrow a\Delta s$ where a is a constant increment, $0 < a < 1$. As a rule we used values $0.5 \leq a \leq 0.95$. For $a = 0.5$ the sequence is $\Delta s = 1, 0.5, 0.25$, etc as was the case in the work [10]. Gradual decrease of Δs provides finetuning values of S_{ik} in each succeeding sweep with increasing accuracy.

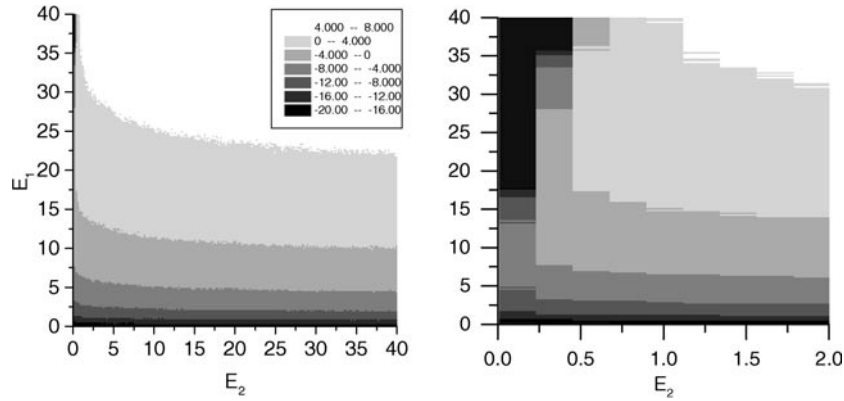


Figure 1. (a) Entropy distribution in the (E_1, E_2) plane presented as a density map. Simulation conditions: number of beads $n = 5$, $E_{\max 1} = E_{\max 2} = 40$, $N_{b1} = N_{b2} = 200$, number of sweeps = 80, length of a sweep $m = 8 \times 10^6$; (b) a part of (a) on an extended E_2 scale.

In order to determine an optimal regime of simulations, we calculated the rates of visits to separate (i, k) cells (by normalization values of $nv(i, k)$) and determined their relative mean square deviation from the homogeneous ('ideal') distribution $p_0 = (N_{b1}N_{b2})^{-1}$. It appeared that change of the relative deviation during a single run strongly depends on the value of the increment a . For example, for $a = 0.5$ (value used in [10, 11]) the relative deviation falls rather fast, from several tens of per cent to about ten per cent, during first few sweeps; then this process stops and a stage of random fluctuations usually follows with relative deviations within 10–20%. For values of a closer to unity, a similar process goes slower but the level of stabilization is lower. For $a = 0.8$, this level was about 1–3%, for $a = 0.95$ it reached 0.3%. The regime of convergence can also be considerably influenced by the length of a sweep m and its increase from the current sweep to the next one. By observing and analysing such simulation phenomena, it is possible to choose an optimal set of input parameters for obtaining the highest possible accuracy.

3. Results and discussion

Our result for the distribution of entropy for $n = 5$ is presented in figure 1. As long as the zero level of S is not important for obtaining averages, we subtract from the entropy distribution values, S_{ik} , the average increase per cell, $m\Delta s/(N_{b1}N_{b2})$, after each sweep. Thus the entropy is normalized so that its mean value over the square in the (E_1, E_2) plane, figure 1, is zero. It is seen that, as a whole, entropy increases with the increase of both E_1 and E_2 . At small E_1 and large E_2 , the isolines run almost parallel to the E_2 axis while at small E_2 the isolines strongly bend to follow the direction of the E_1 axis. We can consider the graph in figure 1 also as that for the density of states, $\Omega(E_1, E_2)$; in this case the levels $-16, \dots, 0, \dots, 8$ should be read as $e^{-16}, \dots, 1, \dots, e^8$.

Having obtained the entropy surface distribution, we can easily calculate canonical surface distributions $P(E_1, E_2; \beta)$ for any temperature. In figure 2 we present the function $\ln P(E_1, E_2; \beta) = -E_1/\beta - E_2\beta + S(E_1, E_2)$ for five values of β , $\beta = \frac{1}{8}, \frac{1}{2}, 1, 2, 8$, covering a wide range of temperatures. The method of presentation is the same as for the entropy in figure 1. It is seen that for the highest temperature ($\beta = \frac{1}{8}$) the maximum of the distribution is stretched along the E_2 axis in a very narrow stripe, isolines are practically parallel to the

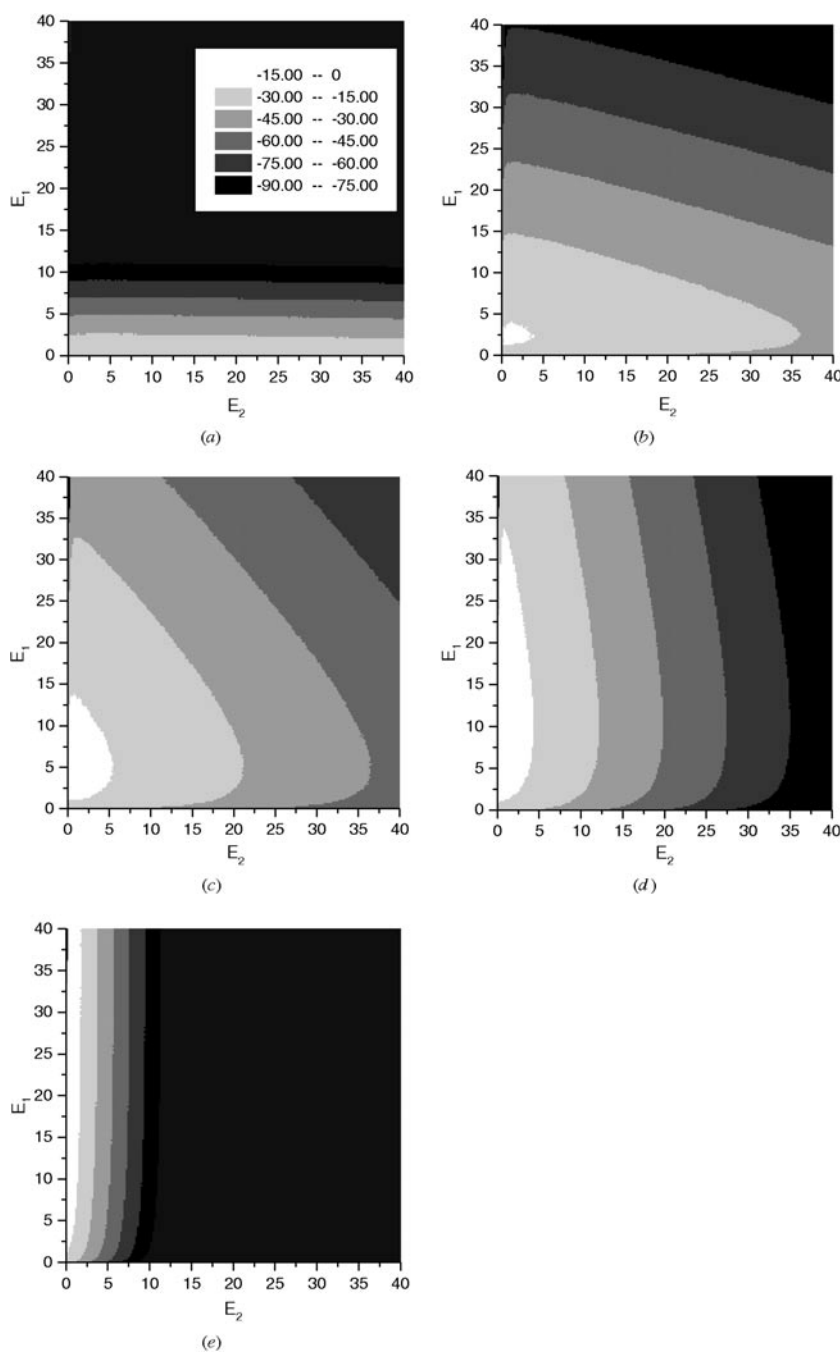


Figure 2. Canonical distributions in the (E_1, E_2) plane for five inverse temperatures β . Presentation and simulation conditions are the same as in figure 1. Values of $\beta : \frac{1}{8}, \frac{1}{2}, 1, 2, 8$ for (a), (b), (c), (d) and (e) respectively.

E_2 axis almost in the whole range of E_2 and the slope of the distribution is very steep. These features correspond to a high-temperature regime (at this temperature quantum and classical results for energy differ only by 0.12%). For $\beta = \frac{1}{2}$, a strong shift of the distribution maximum

Table 1. Calculated average potential energies, $\langle U_p \rangle^{\text{calc}}$, of a three-dimensional quantum harmonic oscillator at different temperatures in comparison with the exact analytical results for the quantum potential energy $\langle U_p \rangle^{\text{exact}}$ and its n -bead approximation $\langle U_p \rangle_n^{\text{exact}}$ for $n = 5$ and 8. Simulation parameters for $n = 5$ are the same as in figures 1 and 2 while for $n = 8$, $E_{\text{max}1} = 70$ and $N_{b1} = 350$.

β	1/8	1/4	1/2	1	2	4	8
$\langle U_p \rangle_5^{\text{calc}}$	11.249	6.007	3.059	1.631	0.975	0.715	0.548
$\langle U_p \rangle_5^{\text{exact}}$	12.0150	6.030	3.060	1.617	0.969	0.725	0.586
$\langle U_p \rangle_8^{\text{calc}}$	11.307	6.025	3.062	1.618	0.972	0.741	0.608
$\langle U_p \rangle_8^{\text{exact}}$	12.0156	6.030	3.0612	1.6207	0.9785	0.7559	0.6714
$\langle U_p \rangle^{\text{exact}}$	12.0156	6.031	3.062	1.623	0.985	0.778	0.751

to the origin of the (E_1, E_2) plane is observed, the isolines are oblique to both axes and the steepness of the slopes is less than before. For $\beta = 1$ the maximum shifts still further towards the E_1 axis and the isolines in most of the square follow at nearly equal angles to both axes. For $\beta = 2$ and 8 we observe a further change of the picture with the maximum canonical distribution being stretched along the E_1 axis especially strongly for the lowest temperature.

The quantity which can be most easily obtained from our entropy distribution by numerical integration and then compared with the exact data is the average potential energy $\langle U_p \rangle$. For the quantum oscillator $\langle U_p \rangle^{\text{exact}} = \frac{d}{4} \coth\left(\frac{\beta}{2}\right)$. The finite n -bead expression for $\langle U_p \rangle$ can also be evaluated analytically (see the appendix). For $n = 5$ this expression reads

$$\langle U_p \rangle_5^{\text{exact}} = d \frac{\beta}{4n^2} \frac{5(16C^4 - 12C^2 + 1)}{16C^5 - 20C^3 + 5C - 1} \quad (7)$$

where

$$C = 1 + \frac{1}{2} \left(\frac{\beta}{n} \right)^2. \quad (8)$$

The comparison with both sets of analytical data is given in table 1.

For inverse temperatures $\beta = \frac{1}{4}, \frac{1}{2}, 1$ and 2 we see that the error of numerical results is within 1.0%. For these temperatures, the essential maximum of the canonical energy distribution is well within the considered (E_1, E_2) area and all relevant configurations are sampled properly. The statistical uncertainty due to finite length of the MC run is evaluated as well within 0.1% for all temperatures; some systematic error may also come from the finite grid on the (E_1, E_2) plane.

For the highest temperature, $\beta = \frac{1}{8}$, the error is about 6%, which is related to a very narrow canonical distribution extended along the E_2 axis and going beyond our cut-off value of $E_{\text{max}2} = 40$ (see figure 2(a)). As long as at $\beta = \frac{1}{8}$, the oscillator is practically classical, we performed an entropy sampling Wang–Landau calculation of the classical density of states, $\Omega(E)$, which in this case is a one-dimensional function. For a classical d -dimensional oscillator there exists an analytical expression for $\Omega(E)$ (see e.g. [15]):

$$\Omega_d(E) = (2\pi)^{d/2} \frac{E^{d/2-1}}{\Gamma(d/2)} \quad (9)$$

which for $d = 3$ yields

$$\Omega_3(E) = 2^{5/2} \pi E^{1/2}. \quad (10)$$

In our entropic sampling calculations with $E_{\text{max}} = 120$ and $N_b = 100$, we reproduced $S_3(E) = \ln \Omega_3(E)$ with very high precision and obtained by means of an appropriate canonical

integration the mean potential energy value $\langle E_p \rangle (\beta = \frac{1}{8}) = 11.995$ which, compared with the exact classical value $\frac{3}{2\beta} = 12$, yields an error less than 0.05 %.

Greater deviations at low temperatures, $\beta = 4$ and 8, are of another nature (though the finite cut-off at $E_{\max 1} = 40$ also plays its role). The canonical distribution in this case is also very narrow and now jammed against the E_1 axis. The principal difference is that in the narrow vicinity of the E_1 axis, there exists a zone inaccessible to the system at finite number of beads n . It is clear that it is impossible to create a path with (almost) zero potential energy E_2 and high bond energy E_1 . This inaccessible region is seen in the upper left part of figure 1(b). It corresponds to the fact that finite-bead approximation of path integral becomes more and more insufficient for obtaining correct results as the temperature decreases. It is evident that, upon increasing the number of beads n , this inaccessible region becomes narrower but does not disappear completely at any finite n . The important point for obtaining accurate results is, however, whether the essential maximum of the canonical distribution overlaps the inaccessible region.

For $\beta = 4, 8$, values of $\langle U_p \rangle_5^{\text{exact}}$ deviate considerably from those of $\langle U_p \rangle^{\text{exact}}$, especially for $\beta = 8$, due to insufficiency of the $n = 5$ bead approximation of the path integral at low temperatures. The deviation of numerical data from $\langle U_p \rangle_5^{\text{exact}}$ is 1.5% and 6% correspondingly.

An additional calculation has been performed for the number of beads $n = 8$. In this simulation, the cut-off energy $E_{\max 1}$ was increased to 70 because the total energy of ‘springs’ scales approximately as n . Yet again, we reached a very good precision of 1% or less in the range of ‘moderate’ temperatures $\beta = 1/4 \dots 2$. One can also see that increasing the number of beads substantially improves results in the low-temperature region, the improvement being of about the same size as one can expect from the analytical result for the finite-bead approximation at $n = 8$.

4. Conclusion

In this communication we have extended the entropic sampling Monte Carlo method within the Wang–Landau algorithm to the case of path integral representation of a quantum system. We have shown that the method in a single simulation run provides reasonably accurate estimation of the energy within a wide temperature range for a quantum particle in a harmonic potential. The presented diagrams of entropy and canonical probability distribution can give a clear indication of whether the simulation parameters (number of beads, cut-off energies, grid resolution) are adequate for the considered problem and what should be done to improve the accuracy. The method can be applied practically without changes for a general case of many particles interacting by an arbitrary potential. All the variety of physical systems contains in different forms of $\Omega(E_1, E_2)$. The account of exchange for identical particles yields another field for applying such methods.

Acknowledgments

This work was supported by the Russian Foundation for Basic Research (RFFI) and the Swedish Research Council (Vetenskapsrådet).

Appendix. Finite n -bead expression for the partition function of a quantum oscillator

The n -bead approximation for the partition function (1) in the case of a one-dimensional quantum oscillator can be presented as

$$Z_n(\beta) = \left(\frac{n}{2\pi\beta}\right)^{n/2} \int dx_1 \cdots dx_n \exp \left[-\left(\frac{n}{\beta} + \frac{\beta}{2n}\right) \sum_i (x_i)^2 + \frac{n}{\beta} \sum_i x_i x_{i+1} \right] \quad (\text{A.1})$$

with cyclic condition, $x_{n+1} = x_1$. Introducing new variables $y_i = \sqrt{\frac{n}{2\beta}} x_i$, we get

$$Z_n(\beta) = \frac{1}{\pi^{n/2}} \int dy_1 \cdots dy_n \exp \left[-\left(2C \sum_i (y_i)^2 - 2 \sum_i y_i y_{i+1}\right) \right] \quad (\text{A.2})$$

where

$$C = 1 + \frac{1}{2} \left(\frac{\beta}{n}\right)^2.$$

For the canonical average potential energy it straightforwardly follows

$$\langle U_p \rangle_n = -\frac{\beta}{2n^2} \frac{dZ_n}{dC} \frac{1}{Z_n}. \quad (\text{A.3})$$

Following the appendix in [14] we can present a bilinear form over y_i in the exponent of (A.2) as a scalar product $(\mathbf{A}_n \mathbf{y} \cdot \mathbf{y})$ where $\mathbf{y} = (y_1 \cdots y_n)$ is an n -dimensional vector and \mathbf{A}_n is the following matrix:

$$\mathbf{A}_n = \begin{pmatrix} 2C & -1 & 0 & \dots & 0 & -1 \\ -1 & 2C & -1 & 0 & \dots & 0 \\ 0 & -1 & 2C & -1 & \dots & 0 \\ \vdots & & & \dots & \dots & \vdots \\ 0 & \dots & 0 & -1 & 2C & -1 \\ -1 & 0 & \dots & 0 & -1 & 2C \end{pmatrix}$$

Reducing the bilinear form to a quadratic form, we express Z_n as

$$Z_n = \frac{1}{\pi^{n/2}} \int dt_1 \cdots dt_n \exp \left(-\sum_i \lambda_i t_i^2 \right) = (\lambda_1 \cdots \lambda_n)^{-1/2} = (\det \mathbf{A}_n)^{-1/2} \quad (\text{A.4})$$

where λ_i are eigenvalues of matrix \mathbf{A}_n . For the determinant of the matrix \mathbf{A}_n , we have

$$\det \mathbf{A}_n = 2(C \Delta_{n-1} - \Delta_{n-2} - 1) \quad (\text{A.5})$$

where Δ_n is the determinant of the matrix

$$\Delta_n = \det \begin{pmatrix} 2C & -1 & 0 & \dots & 0 & 0 \\ -1 & 2C & -1 & 0 & \dots & 0 \\ 0 & -1 & 2C & -1 & \dots & 0 \\ \vdots & & & \dots & \dots & \vdots \\ 0 & \dots & 0 & -1 & 2C & -1 \\ 0 & 0 & \dots & 0 & -1 & 2C \end{pmatrix}.$$

For Δ_n the following relation is valid:

$$\Delta_n = 2C \Delta_{n-1} - \Delta_{n-2} \quad (\text{A.6})$$

Now following (A.3) we obtain for $\langle U_p \rangle_n$:

$$\langle U_p \rangle_n = \frac{\beta}{4n^2} \frac{d \det \mathbf{A}_n}{dC} \frac{1}{\det \mathbf{A}_n}. \quad (\text{A.7})$$

Using (A.5) and (A.6) we can obtain $\det \mathbf{A}_n$ recursively for any finite value of n .

For $n = 5$ we get

$$\det \mathbf{A}_5 = 32C^5 - 40C^3 + 10C - 2.$$

For $\langle U_p \rangle_5$ it now yields

$$\langle U_p \rangle_5 = \frac{\beta}{4n^2} \frac{5(16C^4 - 12C^2 + 1)}{16C^5 - 20C^3 + 5C - 1}. \quad (\text{A.8})$$

At high temperatures this expression gives the classical limit

$$\langle U_p \rangle_5 = \frac{1}{2\beta}.$$

At low temperatures it goes to zero due to the finite value of n .

The mean potential energy for $n = 8$ is

$$\langle U_p \rangle_8 = \frac{\beta}{4n^2} \frac{32C^7 - 48C^5 + 20C^3 - 2C}{4C^8 - 8C^6 + 5C^4 - C^2}. \quad (\text{A.9})$$

The generalization to the d -dimensional case is straightforward.

References

- [1] Lyubartsev A P, Martsinovski A A, Shevkunov S V and Vorontsov-Velyaminov P N 1992 *J. Chem. Phys.* **96** 1776
- [2] Nezbeda I and Kolafa J 1991 *Mol. Simul.* **5** 391
- [3] Attard P 1993 *J. Chem. Phys.* **98** 2225
- [4] Kaminsky R D 1994 *J. Chem. Phys.* **101** 4986
- [5] Marinari E and Parisi G 1992 *Europhys. Lett.* **19** 451
- [6] Hukushima K and Nemoto K 1996 *J. Phys. Soc. Japan* **65** 1604
- [7] Berg B A and Neuhaus T 1992 *Phys. Rev. Lett.* **68** 9
- [8] Lee J 1993 *Phys. Rev. Lett.* **71** 211
- [9] Iba Y 2001 *Int. J. Mod. Phys.* **12** 623
- [10] Wang F and Landau D P 2001 *Phys. Rev. Lett.* **86** 2050
- [11] Wang F and Landau D P 2001 *Phys. Rev. E* **64** 056101-1
- [12] Feynman R P 1972 *Statistical Mechanics* (New York: Benjamin)
- [13] Barker J A 1979 *J. Chem. Phys.* **70** 2914
- [14] Vorontsov-Velyaminov P N, Nesvit M O and Gorbunov R I 1997 *Phys. Rev. E* **55** 1979
- [15] Kubo R 1965 *Statistical Mechanics. An Advanced Course With Problems and Solutions* (Amsterdam: North-Holland)